Modeling of Casting, Welding, and Advanced Solidification Processes - XII
Edited by: Steve L. Cockcroft and Daan M. Maijer
TMS (The Minerals, Metals & Materials Society), 2009

Modeling Nucleation and Growth of Zinc Grains in Hot-Dip Galvanized Coatings

Aurèle Mariaux[1], Tom Van De Putte[2] and Michel Rappaz[1]

[1]Computational Materials Laboratory, Ecole Polytechnique Fédérale de Lausanne; CH-1015 Lausanne, Switzerland
[2]ArcelorMittal Research Industry Gent; B-9060 Zelzate, Belgium

Keywords: cellular automaton, steel, hot-dipping, dendritic growth

Abstract

Hot-dip galvanized Zn-0.2wt%Al coatings on steel sheets exhibit a strong basal texture ($\{0001\}$ parallel to the sheet plane). Part of this texture can be explained by the faster growth of $\langle 10\bar{1}0\rangle$ dendrites as compared with $\langle 0001\rangle$, granting basal grains (*i.e.* grains with their basal plane parallel to the sheet) a larger extension than others. But Sémoroz *et al.* [1] showed that the fraction of basal grains itself is also higher than its value in a population of randomly oriented grains. This indicates that more basal grains nucleate during the early stages of solidification.

In order to study the nucleation parameters of Zn on a steel substrate, a coupled cellular automaton (CA) - finite volume (FV) model was developed. The CA simulates microstructure formation in the coating, while the FV part considers heat diffusion in the coating and in the substrate. 3D phase field computations accounting for the 6-fold symmetry of Zn and for wetting on the coating boundaries, are being performed to refine the dendrite growth kinetics law implemented in the CA. On the experimental side, the grain orientation distribution was measured by EBSD in industrial galvanized coatings remolten in an infrared image furnace and solidified at different cooling rates. The nucleation parameters of Zn in the coating were determined from this data by inverse modeling, using the coupled model.

Introduction

In hot dip galvanization, steel sheets are continuously immersed in a bath of molten zinc at a speed of about 1 m/s. At bath exit, a thin film of liquid alloy, typically 10 μm thick, is carried along on the steel surface, due to capillarity. During subsequent cooling, the film transforms into a solid layer, which provides very effective corrosion protection to the steel substrate.

The solidification microstructure has a strong influence on the mechanical properties of the coating. It is usually made of large grains, called spangles, with a diameter of several hundreds of micrometers, or even millimeters. It also exhibits a strong basal texture ($\{0001\}$ parallel to the sheet surface) [1, 2]. This can be partly explained by the mechanisms of dendritic growth in the hcp Zn system: $\langle 10\bar{1}0\rangle$ dendrites in the basal plane grow at about 30% higher speeds than $\langle 0001\rangle$ dendrites [3]. If the grain has a basal orientation, all of its six $\langle 10\bar{1}0\rangle$ dendrites are well aligned with the coating plane and can grow freely. If the crystal is rotated, its fast dendrites very early impinge onto the film boundaries (substrate and free surface) and their growth is slowed down. Therefore, basal grains can become larger than grains with any other orientation.

However, this is not the only reason for such a texture: neglecting the size of individual grains, the number of basal grains is significantly higher than that predicted for a random

orientation distribution. The small thickness of the coating, combined with the abundance of nucleation sites at its boundaries, indicates that nucleation is heterogeneous, probably on these two surfaces. As grains keep their orientation during growth, this means that not only growth, but also nucleation participates to the texture formation: nuclei with their basal plane parallel to the substrate are more numerous.

Heterogeneous nucleation in real castings can be described as an athermal nucleation process, as described for example by Thévoz *et al.* [4, 5]. In this model, a given population of nucleation sites are present, each of them producing a new grain if its critical undercooling is exceeded and if it is still in contact with the liquid. Therefore, knowing the thermal history of a sample and the growth kinetics of dendrites, the final grain structure can be predicted from the initial population of nucleation sites.

In order to study nucleation in hot dipped coatings, a two-fold approach was developed, combining experimental measurement of the influence of cooling conditions on the final grain orientation distribution, and numerical simulation of the solidification process. This enabled a precise determination of the nucleation parameters, including both the crystallographic orientation of the nuclei and the distribution of their critical undercooling.

Experiments

In order to measure the grain number and orientation distribution as a function of the cooling conditions, samples of industrially galvanized steel sheets were reheated up to 450°C very quickly in an infrared (IR) image furnace. After remelting, the specimen was cooled down using a specifically designed air blowing system [6], in a range from -1 to -30 K/s. After cooling, the number of grains per unit area and their orientation distribution in each specimen were measured using Electron Backscatter Diffraction (EBSD).

The cooling curve and grain orientation distribution obtained at intermediate cooling rate are shown in figures 1 and 2, respectively. If the orientation of the grains were totally

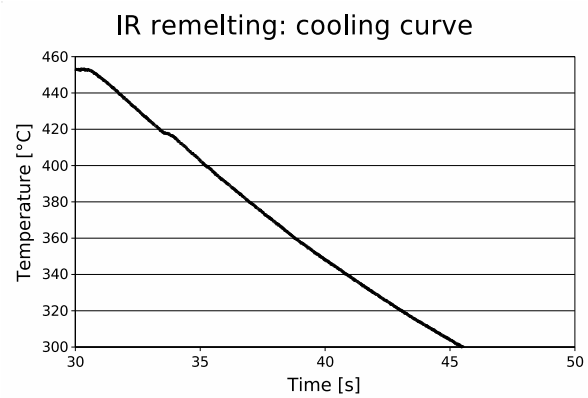

Figure 1: Temperature curve of a 20 μm thick Zn-0.2%Al-0.02%Fe coating deposited on a 800 μm steel sheet, recorded during cooling at a cooling rate of -12 K/s in an IR image furnace after remelting. A small solidification plateau can be seen sightly below 420 °C.

random, the distribution of the angle, θ, between $\{0001\}$ and the sheet plane would be proportional to $(\sin\theta)$. It is the case above 30°, but not below this value, where the bars are much higher, indicating a preferential nucleation orientation. In order to quantify this discrepancy, a $(\sin\theta)$ curve was fitted to the bars above 30° in figure 2. The integral of this function from 0 to 90° gave the number of grains that fitted into this random distribution.

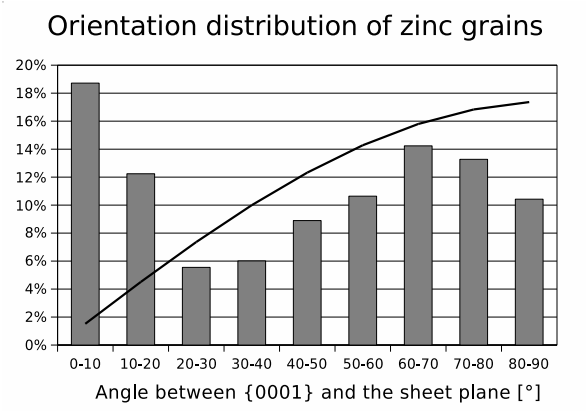

Figure 2: Histogram of the grain orientation in the specimen whose cooling curve is shown in figure 1. The excess basal grains are visible in the large peaks at low angles. The theoretical distribution for a random population is shown with a continuous line for comparison.

The number of remaining grains below 30° were considered to belong to a basal population. The total number of grains and the ratio of the basal to the random population were taken as characteristics of the measured grain orientation distributions.

Modeling

In order to model the cooling process during hot dipping or during the IR furnace remelting experiments, the substrate and the coating must be treated in different ways. The former undergoes no phase transformation and can be considered as an inert heat conductive mass, while the latter is the actual solidifying medium. However, the coating is so thin compared to the steel sheet (a least a factor 10-20) that it makes only a negligible contribution to the heat diffusion process: the temperature difference across it is negligible and its temperature can be considered as equal to that of the substrate. The coating therefore reduces to a latent heat source at the boundary of the steel sheet.

A new model was developed, considering this particular geometry, based on the CAFE approach of Gandin *et al.* [7] for bulk specimen and on that of Sémoroz *et al.* [3] for thin isothermal coatings. Heat diffusion is treated by a finite volume (FV) model of the substrate, while a cellular automaton (CA) model is used for the simulation of coating solidification. Both are solved alternately in a coupled way: the FV supplies the temperature distribution in the coating to the CA, which in turn gives back the repartition of the solid, mushy and liquid regions to the FV, and thus the latent heat release.

A sketch of the model is shown in figure 3. The meshes were simplified using some geometrical considerations. First, since the sheet is coated on its two surfaces, only half is modeled. Additionally, thermal gradients are present in the sheet in only two directions: across its thickness (z) and along its displacement direction (y). Along x, it can be considered as isothermal. Thus, no heat diffusion computation is needed in this direction and the FV heat diffusion model is only 2D.

Coating model: CA

A similar model had already been developed by Sémoroz *et al.* [3], but only for isothermal samples. The CA of the present model is largely inspired from their work. The cell mesh

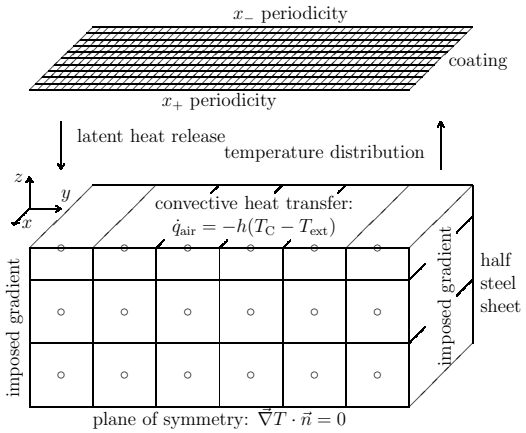

Figure 3: Geometry of the coupled CA-FV model.

is two-dimensional, in the sheet plane (xy). Since the sheet is invariant in x, a periodic boundary condition is set at the x_- and x_+ boundaries. Along y, none is set: grains that reach the end of the domain are simply stopped. At each time step, the coating model performs the following operations: create new grains with the nucleation algorithm, update all dendrite tip positions and identify the cells which are captured by the growth of the dendrites. The individual steps are detailed below.

Nucleation. An athermal nucleation model is used: nucleation sites are generated at the beginning of the computation, each with an activation undercooling and an orientation (given by the Euler angles ϕ_1, Φ and ϕ_2). Then, a new grain is created at every nucleation cell whose critical undercooling has been reached, provided it has not yet been captured by another grain.

As described above, the orientation distribution of the grains can be decomposed into a basal and a random part, whose relative amounts change with cooling rate. In order to be able to reflect these observations, the population of nucleation sites is also made of two subgroups with their own distribution of orientation and undercooling. In the basal group, the second Euler angle Φ (equal to the angle between $\{0001\}$ and the sheet plane) is distributed from 0 to 22.5° with a density proportional to $\cos(4\Phi)$. In the random group, Φ ranges from 0 to 90° with a probability proportional to $\sin\Phi$. In both groups, ϕ_1 and ϕ_2 are chosen uniformly in the intervals $[0°; 360°]$, respectively $[0°; 60°]$ (due to the 6-fold symmetry of zinc).

The critical undercooling is modeled in the same way in both groups: starting at a minimal undercooling, ΔT_{min}, the cumulative distribution of active nuclei increases linearly up to a maximum ΔT_{max} where it reaches a maximum value, n_{nuc}. These three parameters ΔT_{min}, ΔT_{max} and n_{nuc} have different values for the two nucleation sites populations.

Dendritic growth. Two factors affect dendrite speed: the undercooling and impingement with the film boundaries. Thus

$$v = v_{\text{IMS}}(\Delta T) \cdot \text{INC}(\alpha) \tag{1}$$

The first factor in this equation is the speed of a free $\langle 10\bar{1}0 \rangle$ dendrite in a bulk alloy. It is computed using a fourth order polynomial fit to Ivantsov's solution with a marginal stability

criterion [8]. The second factor characterizes the slowing effect of the film geometry and the difference between $\langle 10\bar{1}0\rangle$ and $\langle 0001\rangle$ dendrites.

$$\mathrm{INC}_{\langle 10\bar{1}0\rangle}(\alpha) = 1 - b_{\langle 10\bar{1}0\rangle}\alpha \quad (2)$$

$$\mathrm{INC}_{\langle 0001\rangle}(\alpha) = a_{\langle 0001\rangle} - b_{\langle 0001\rangle}\alpha \quad (3)$$

where α is the impingement angle of the dendrite on the interface, $a_{\langle 0001\rangle}$ is the speed ratio between $\langle 0001\rangle$ and $\langle 10\bar{1}0\rangle$ and $b_{\langle ijkl\rangle}$ are coefficients determined by phase field simulations [9].

Cell capture. Cells can be captured in two ways: either by activation of a nucleation site, if they contain one, or by grain growth. The former is straight forward. The latter is done by next-neighbor expansion: to be captured, a cell must be enclosed within the envelope of a grain, and have a neighbor which already belongs to this grain. The second condition ensures that grains grow as a continuous domain. However, it also sets a restriction that dendrite tips may not advance by more than one cell during a single time step.

Substrate model: FV

The heat equation in a x-z plane is implemented using an explicit scheme, which for a node C gives:

$$\rho c_\mathrm{p}\Delta x\Delta y\Delta z\frac{T_\mathrm{C}^{t+\Delta t}-T_\mathrm{C}^t}{\Delta t} = \kappa\left(\Delta x\Delta z\frac{T_\mathrm{E}^t-2T_\mathrm{C}^t+T_\mathrm{W}^t}{\Delta y}+\Delta x\Delta y\frac{T_\mathrm{N}^t-2T_\mathrm{C}^t+T_\mathrm{S}^t}{\Delta z}\right) \quad (4)$$

where W, E, N and S denote the western, eastern, northern and southern neighbors of node C, ρc_p and κ are the volumetric specific heat and the heat conductivity of the substrate, respectively, and Δx, Δy, Δz are the size of the finite volumes.

The following boundary conditions are applied: along the displacement of the sheet, thermal gradients can be imposed on the y_+ and y_- boundaries of the domain to reflect the situation on an industrial galvanizing line. The lower z boundary (core of the sheet) is adiabatic. For a node C on the top surface, the heat diffusion equation contains two more terms associated with air cooling and latent heat release by the coating. One has:

$$\begin{aligned}&\left(\rho_\mathrm{s}c_\mathrm{ps}\frac{\Delta z}{2}+\rho_\mathrm{c}c_\mathrm{pc}e_\mathrm{c}\right)\frac{T_\mathrm{C}^{t+\Delta t}-T_\mathrm{C}^t}{\Delta t}\Delta x\Delta y\\ &\quad=\left(\left(\kappa_\mathrm{s}\frac{\Delta z}{2}+\kappa_\mathrm{c}e_\mathrm{c}\right)\frac{T_\mathrm{E}^t-2T_\mathrm{C}^t+T_\mathrm{W}^t}{\Delta y}-\kappa_\mathrm{s}\frac{T_\mathrm{C}^t-T_\mathrm{S}^t}{\Delta z}\Delta y\right)\Delta x+\dot{q}_\mathrm{air}+\dot{q}_\mathrm{lat}\end{aligned}$$

Air cooling is modeled using a heat transfer coefficient, h:

$$\dot{q}_\mathrm{air} = -h(T_\mathrm{C}^t - T_\mathrm{ext})\Delta x\Delta y \quad (5)$$

The latent heat release for node C is given by

$$\dot{q}_\mathrm{lat} = L_\mathrm{f}e_\mathrm{c}\Delta x\Delta y\frac{g_{\mathrm{s\,C}}^{t+\Delta t}-g_{\mathrm{s\,C}}^t}{\Delta t} \quad (6)$$

where L_f is the volumetric latent heat of the coating and e_c its thickness. The change in solid fraction, g_sc in the finite volume is computed by collocating the contributions of the cells, ν, on a portion, $\partial\Omega_\mathrm{C}$, of the surface:

$$g_{\mathrm{s\,C}}^{t+\Delta t}-g_{\mathrm{s\,C}}^t = \frac{1}{\Delta x\Delta y}\sum_{\nu\in\partial\Omega_\mathrm{C}}\varphi_\mathrm{C}(y_\nu)\delta x\delta y\left(g_{\mathrm{s}\,\nu}^{t+\Delta t}-g_{\mathrm{s}\,\nu}^t\right) \quad (7)$$

where δx, δy is the size of the cells and $\varphi_{\mathrm{C}}(y_\nu)$ the collocation coefficient. In other words, the latent heat released by cell number ν, at position (x_ν, y_ν), is summed with a weighing coefficient $\varphi_{\mathrm{C}}(y_\nu)$ on the two closest nodes of the FV mesh.

The internal solid fraction of the grains, $\tilde{g}_{\mathrm{s}}(T)$, is modeled with a truncated Scheil model [10]. The solid fraction is 0 above the liquidus, T_{liq}, 1 below the eutectic point, T_{eut}, and given by Scheil-Gulliver equation in between:

$$\tilde{g}_{\mathrm{s}}(T) = 1 - \left(\frac{T_{\mathrm{m}} - T}{T_{\mathrm{m}} - T_{\mathrm{liq}}} \right)^{1/(k-1)} \tag{8}$$

where T_{m} is the melting point of pure zinc and k the partition coefficient. The truncation at T_{eut} makes $\tilde{g}_{\mathrm{s}}(T)$ discontinuous, but the FV model needs the first derivative $\mathrm{d}\tilde{g}_{\mathrm{s}}/\mathrm{d}T$ to be defined. Thus, $\tilde{g}_{\mathrm{s}}(T)$ was substituted with a third order polynomial in a small domain around T_{eut} to make the function derivable. $\tilde{g}_{\mathrm{s}}(T)$ is also discontinuous at T_{liq}, but no correction was made, because dendritic solidification always starts at some undercooling below the liquidus.

In modeling the change in solid fraction in a cell, two cases must be distinguished. If the cell was already mushy at the beginning of the time step, its change in solid fraction is only induced by the variation of temperature:

$$g_{\mathrm{s}\,\nu}^{t+\Delta t} = g_{\mathrm{s}\,\nu}^{t} + \left. \frac{\partial \tilde{g}_{\mathrm{s}}}{\partial T} \right|_{T_\nu^t} (T_\nu^{t+\Delta t} - T_\nu^t) \tag{9}$$

Conversely, if it gets captured during the current time step, while its temperature T_ν^t is already below the liquidus, its solid fraction goes from $g_{\mathrm{s}\,\nu}^t = 0$ to

$$g_{\mathrm{s}\,\nu}^{t+\Delta t} = \tilde{g}_{\mathrm{s}}(T_\nu^{t+\Delta t}) \approx \tilde{g}_{\mathrm{s}}(T_\nu^t) + \left. \frac{\partial \tilde{g}_{\mathrm{s}}}{\partial T} \right|_{T_\nu^t} (T_\nu^{t+\Delta t} - T_\nu^t) \tag{10}$$

These two different cases are treated by introducing a parameter, I_ν, indicating whether the cell is liquid ($I_\nu = 0$) or mushy ($I_\nu = 1$).

Results

The model was used to simulate the cooling process in the infrared remelting experiment. This experiment has still a small thermal gradient along the y-direction. As an example, a snapshot of solidification during cooling at -12 K/s is shown in figure 4. A temperature gradient is imposed at the left and right ends of the domain. Due to the resulting temperature difference, solidification is more advanced on the left than on the right, giving an impression of the time evolution of the grain shapes and extensions.

The key information for microstructure prediction in hot dip galvanized coatings is the distribution of nucleation sites. It can be roughly determined from the infrared remelting measurements, but more precise values are needed. Thus, starting from these estimates, the three nucleation parameters (ΔT_{min}, ΔT_{max}, n_{max}) of each distribution were refined by inverse modeling. The discrepancy between simulation and experiment was quantified by comparing the differences in total grain number and in the ratio between the number of basal and random grains. These deviations were then minimized by optimization.

The method converged to the results shown in figure 5. Agreement between experimental and computed values is quite good, except for the number of random grains at -12 K/s. The values obtained for ΔT_{min} are 0.55 K for the basal distribution and 0.7 K for the random one. This agrees with the measurements of Quiroga *et al.* [11]. Preferential nucleation of basal grains is confirmed by the difference between the ΔT_{min} of both distributions: the first basal grains need 0.15 K less undercooling to form, as compared to the first random grains.

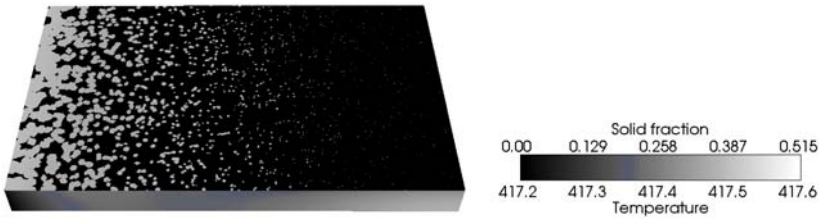

Figure 4: Snapshot of simulation during cooling at -12 K/s. The simulated domain is 5 mm long and 3 mm wide. A positive thermal gradient is imposed from left to right. On the top surface, gray tones indicate the solid fraction in the coating, and in the cross section of the sheet, the temperature distribution in the substrate (or coating).

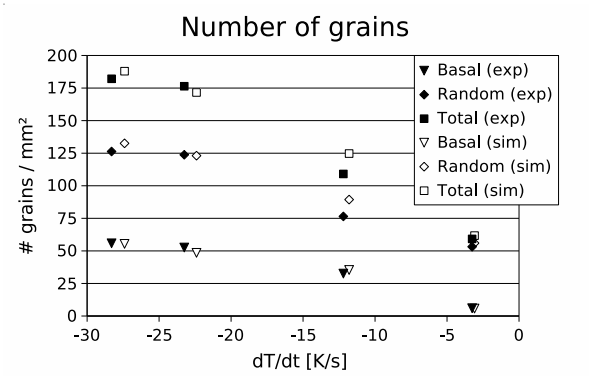

Figure 5: Experimental and simulation results after inverse modeling.

Phase field

In the dendrite growth model of the CA, the treatment of impingement with the film boundaries involves two parameters $b_{\langle ijkl \rangle}$, whose values were determined by phase field modeling (PhF) [9]. However, the model used at that time was only two-dimensional. This puts a strong restriction on solute movement at the tip: if an actual dendrite approaches a wall with a slanting angle, the rejected solute can diffuse away in all directions around it; however in the 2D PhF model, the only escape routes are in the incidence plane of the dendrite onto the wall. This artificially increases solute accumulation and thus dendrite slowing.

A 3D massively parallel PhF model is available at the Computational Materials Laboratory of EPFL. Wetting conditions are presently being implemented into it in such a way to take the high anisotropy of zinc into account. Using this model, the slowing effect of wall impingement on dendrite growth will be computed again. The results will be used to refine the growth algorithm in the coupled CA-FV model and thus obtain more precise values of the nucleation parameters.

Conclusion

Combining three simulation techniques (CA, FV and PhF) and a new experimental device, a very powerful tool has been designed for investigation of nucleation in hot dip galvanization. The special nucleation and growth conditions in a coating geometry were implemented in the model. Although a very simple distribution of activation undercooling has been chosen in the CA, it can accurately predict the experimental microstructure. The minimal under-

cooling obtained by inverse modeling is in agreement with previous measurements reported in literature. Further refinements are being realized to increase precision, including three-dimensional modeling of the impingement of dendrites with the film boundaries, as well as refinement of the orientation and undercooling of the nucleation sites.

Acknowledgements

EBSD measurements were performed at the Centre Interdisciplinaire de Microscopie Electronique of Ecole Polytechnique Fédérale de Lausanne. Financial support of ArcelorMittal is gratefully acknowledged.

References

[1] A. Sémoroz, L. Strezov, and M. Rappaz, "Orientation domains and texture in hot-dipped galvanized coatings", *Metallurgical and Materials Transactions A*, 33A (8) (2002), 2695–2701.

[2] N. J. Wall, J. A. Spittle, and R. D. Jones, "The crystallography of the spangle of hot dipped galvanized coatings on mild steel strip", in *1st International Conference on Zinc Coated Steel Sheet* (Zinc Development Association, 1985), C1.

[3] A. Sémoroz, L. Strezov, and M. Rappaz, "Numerical simulation of Zn coating solidification", *Metallurgical and Materials Transactions A*, 33A (8) (2002), 2685–2694.

[4] M. Rappaz, Ph. Thévoz, Z. Jie, J.-P. Gabathuler, and H. Lindscheid, "Micro-/macroscopic modelling of equiaxed solidification", in *Computer simulation of solidification. E-MRS 1986* (Les Ulis: Les Editions de Physique, 1986), 277–284.

[5] Ph. Thévoz, J.-L. Desbiolles, and M. Rappaz, "Modeling of equiaxed microstructure formation in casting", *Metallurgical Transactions A*, 20A (2) (1989), 311–322.

[6] A. Mariaux, T. Van De Putte, and M. Rappaz, to be published.

[7] Ch.-A. Gandin and M. Rappaz, "A coupled finite element—cellular automaton model for the prediction of dendritic grains structures in solidification processes", *Acta Metallurgica et Materialia*, 42 (7) (1994), 2233–2246.

[8] M. Rappaz, S. A. David, J. M. Vitek, and L. A. Boatner, "Analysis of solidification microstructures in Fe-Ni-Cr single-crystal welds", *Metallurgical transactions A*, 21A (1990), 1767–1782.

[9] A. Sémoroz, S. Henry, and M. Rappaz, "Application of the phase-field method to the solidification of hot-dipped galvanized coatings", *Metallurgical and Materials Transactions A*, 31A (2) (2000), 487–495.

[10] J.D. Hunt, "Steady state columnar and equiaxed growth of dendrites and eutectic", *Materials Science and Engineering*, 65 (1984), 75–83.

[11] A. Quiroga, S. Claessens, B. Gay, and M. Rappaz, "A novel experiment for the study of substrate-induced nucleation in metallic alloys: Application to Zn-Al", *Metallurgical and Materials Transactions A*, 35A (11) (2004), 3543–3550.